ULB-TH/01-13

Prompt Atmospheric Neutrinos: Phenomenology and Implications [1]

C.G.S. Costa and C. Salles

Service de Physique Théorique, CP 225, Université Libre de Bruxelles, Boulevard du Triomphe, 1050 Brussels, Belgium

Abstract

We present an overview of the phenomenology of prompt neutrinos produced in the atmosphere by the decay of charmed particles. In face of the great activity involving operational and proposed large scale neutrino telescopes, we discuss the implications of different scenarios in calculating the prompt flux, upon the detectable signals in these experiments.

[1] Talk presented at the *PHENO 2001 Symposium*, May 7-9, 2001, University of Wisconsin - Madison. http://pheno.physics.wisc.edu/pheno01/

1 Introduction

One could imagine to build a special kind of experimental facility to study high-energy and very-high-energy neutrinos. While on the wishful thinking, one could gather all the best conditions. Desirable characteristics include:

- to provide acceleration of parent particles up to the highest energies;
- to be coupled to the largest particle beam dump;
- to be shielded by a set of the largest and most dense absorbers available;
- to be monitored by an ensemble of several detectors, each operated with a different detection technique, and complementary acceptances; and
- to produce and detect neutrinos covering a broad range of energies, perhaps from 10^6eV to 10^{18}eV.

Does it sounds like a too difficult enterprise? Well, we get very close to it, if we regard all cosmic-ray phenomena and corresponding experiments in a complementary way.

Think of several cosmic particle acceleration mechanisms, provided by sources such as supernova explosions, neutron stars in binary systems, active galactic nuclei, gamma-ray bursts, pulsars, rapidly spinning magnetars and yet some exotic objects (topological defects, decaying massive relics). Choose as target our planet, where gravitationally trapped gaseous elements serve as a beam dump, and the solid core material, from one surface to the other, provide at the same time shielding and support for different purpose detectors, scattered around at different heights and depths. A block diagram of this "ultimate" high-energy facility looks like:

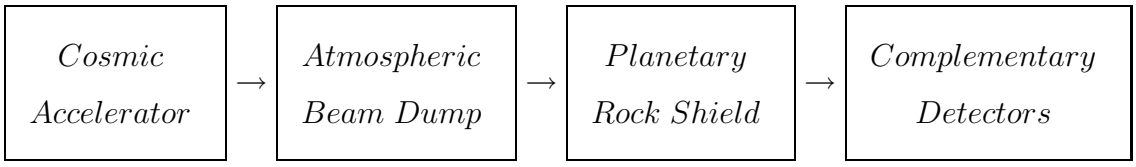

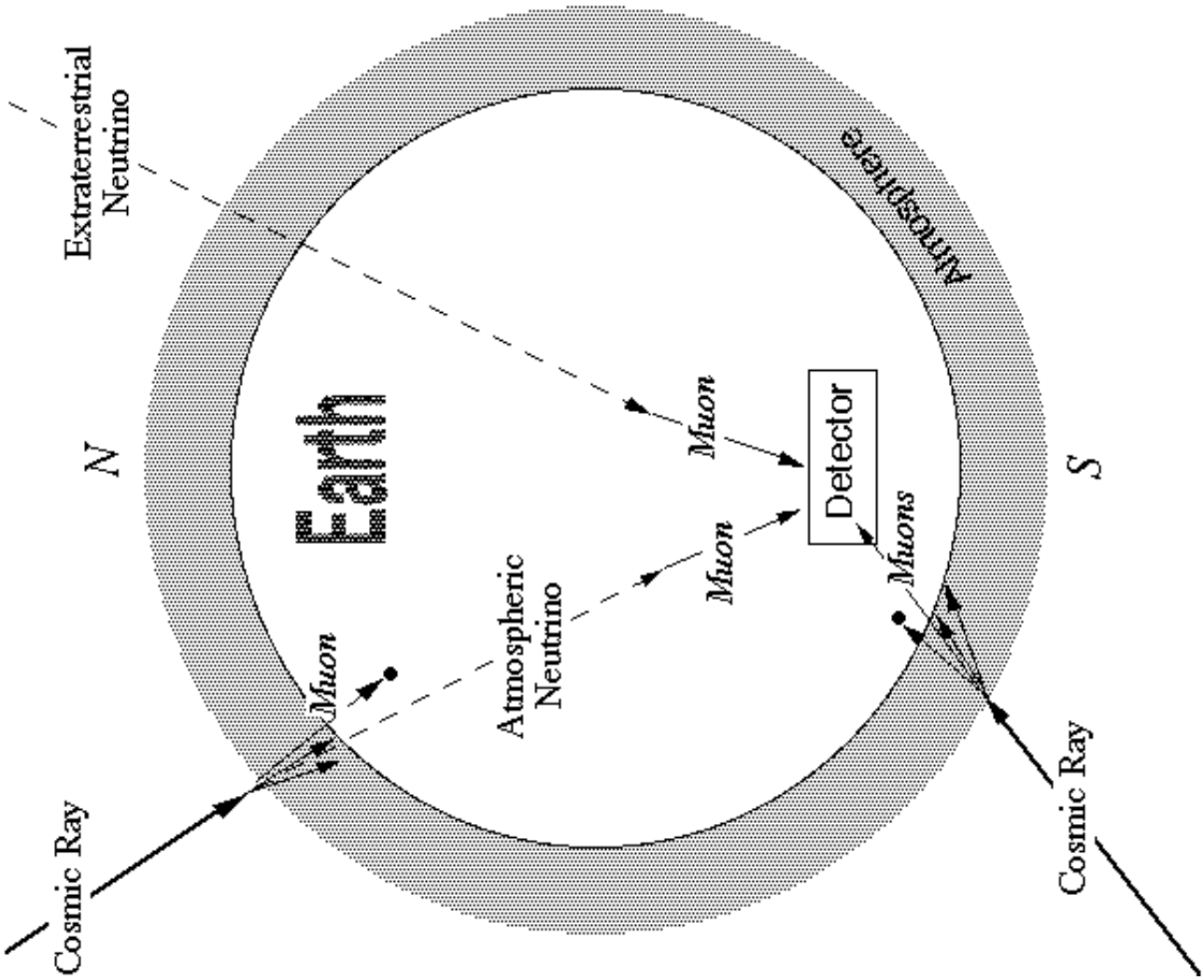

Fig. 1. Sketch of the "ultimate" experimental neutrino facility (the Cosmos included!).

A more realistic sketch for this omnipresent experimental neutrino facility is presented in Figure 1. One should consider the whole cosmos as part of the figure. One may also include several detectors scattered around, with different and complementary purposes, for example: optical and gamma-ray space telescopes; primary cosmic-ray satellite and balloon borne calorimeters; mountain-altitude cosmic-ray family emulsion chamber detectors; cherenkov, fluorescence and particle extensive air shower detectors; muon magnetic spectrometers; and yet large underground, underwater and under-ice observatories.

High-energy extraterrestrial neutrinos (above tens of TeV) may be directly produced at the same (galactic or extra-galactic) sources of high-energy cosmic-ray particles and gamma-rays, including those of the highest energies. Low energy neutrinos (below tens of MeV) are produced directly in nuclear reactions at the core of the Sun.

Intermediate energy neutrinos are produced locally, at the planetary scale. A cosmic accelerated primary particle, a nucleon for example, impinging upon nuclei of air in the atmosphere, will generate a shower of secondary particles, which may propagate to the ground or even below. The main contributions to air showers come from the prodution of a) neutral pions, giving rise to electromagnetic cascades (a sequence of photons and electron-positron pairs); and of b) charged mesons (mainly pions and kaons), giving rise to hadronic cascades. Charged-meson decays will give rise to neutrinos and muons; these muons on their turn may eventually decay into neutrinos, all contributing to what is called the *conventional atmospheric neutrino flux*[1].

The semileptonic decay of heavy quark particles, produced in the hadronic cascades initiated by cosmic-ray interactions, also gives rise to atmospheric neutrinos, a particular set known as the *prompt atmospheric neutrino flux*.

These prompt neutrinos are the subject of the present talk. Among the motivations for their study, we highlight the following:

- High Energy Neutrino Telescopes -
  Though neutrinos are the most abundant cosmic rays at sea level, their measurement requires large underground detectors, in order to compensate for the small neutrino-nucleon cross section. Nowadays operational neutrino telescopes, like AMANDA[2] and BAIKAL[3], are taking and analizing data. They are being optimized to increase signal, data statistics and energy coverage, and to reduce the background, mainly caused by muons and by electronics limitations. Other similar and much larger instruments are being contemplated (Antares, Nestor, Nemo, IceCube)[4]. As will be shown later, there is the possibility that prompt neutrinos are observable in such neutrino detectors[5].
- Background to Cosmic Neutrinos -
  The measurement of galactic and extra-galactic neutrinos, which is the main purpose of neutrino telescopes, is of course limited by discrimination against atmospheric neutrinos, the prompt component included.
- Bounds to Charm Production Cross Section -
  The actual measurement of prompt neutrinos, or the failure to do so, will impose constrains to the charm production cross section at high energy[6], in a similar way as it has been done through the investigation of muon poor horizontal air showers[7].
- Proton Small-x Gluon PDF -
  It has been shown that the spectral index of the prompt atmospheric neutrino flux may depend linearly on the slope of the gluon distribution function at very small x, not reachable at colliders[8].
- Background to High Energy Neutrino Oscillations -
  Prompt decay of the charm-strange meson D_s provide the unique *direct* source of high-energy tau-neutrinos in the atmosphere, which may compete

with those coming from flavor oscillation of atmospheric or extraterrestrial muon-neutrinos[5].

Why charm turns out to be of such particular interest to the study of high energy neutrinos?
The answer comes easily from the analysis of the *critical energy* of different neutrino-parent particles produced in cosmic-ray interactions in the atmosphere. The critical energy delimits the competition between decay and interaction lengths, that is to say, above this energy the parent particle is likely to interact or be slowed down, rather than to decay into a neutrino. Table 1 compares the critical energies calculated for muons, pions and kaons (parents of the conventional atmospheric neutrino flux) and for relevant charm baryons and mesons (parents of the prompt flux). While the contributions of the conventional component to the neutrino flux are constrained below 1 TeV, the charm prompt decays - although less copious - represent the *only* atmospheric contribution up to around 100,000 TeV.

In what follows we present an outline of the calculation of the prompt neutrino component in the atmosphere, comparing different phenomenological approaches found in the literature. Next we discuss the implications of the different prompt flux scenarios upon the detectable signals in large scale neutrino telescopes.

Table 1
Critical energies ε_{critic} of selected particles.

Particle	Elementary contents	mc^2 (MeV)	ε_{critic} (GeV)
μ^+, μ^-	lepton	106	1.0
π^+, π^-	$u\bar{d}, \bar{u}d$	140	115
K^+, K^-	$u\bar{s}, \bar{u}s$	494	855
Λ^o	uds	1116	9.0×10^4
D^+, D^-	$c\bar{d}, \bar{c}d$	1870	3.8×10^7
$D^o, \bar{D}^o$	$c\bar{u}, \bar{c}u$	1865	9.6×10^7
D_s^+, D_s^-	$c\bar{s}, \bar{c}s$	1969	8.5×10^7
Λ_c^+	udc	2285	2.4×10^8

2 Calculation

The particle and energy flow along the development of an air shower, at different atmospheric depths x (given in units g/cm^2), relevant for the production of prompt leptons, can be summarized as:

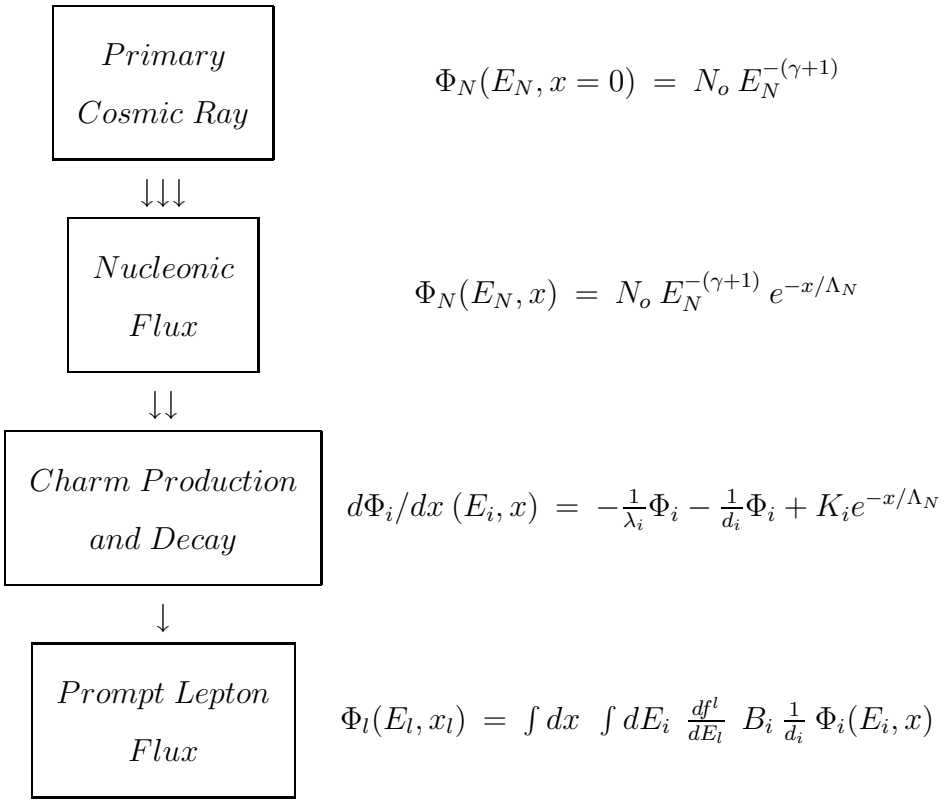

The index N stands for the nucleons (protons, neutrons) arriving at the top of the atmosphere ($x = 0$), with differential energy spectrum Φ_N described by a power law. They cascade down, subjected to an attenuation length Λ_N, to a generic level x where they may produce a charmed particle of type-i ($i = D^{\pm}, D^o, \bar{D}^o, D_s^{\pm}, \Lambda_c^+$). The term K_i is related to the charm production spectrum-weighted moment Z_{Ni}, while λ_i and d_i are respectively the charm interaction and decay lengths. Finally, upon decay of the charmed particle to produce the lepton l, with branching ratio B_i and decay spectrum df^l/dE_l, we have calculated the differential flux of prompt leptons $\Phi_l(E_l, x_l)$, with energy E_l at atmospheric depth x_l.

Detailed calculation of the prompt lepton component is presented in Ref.[9]. In order to have a taste of what this result may look like, and what it signifies, we write down an approximate solution, valid for energies below the charm

critical energy and for depths of the the order of the whole atmosphere:

$$\Phi_l(E) \approx \quad Z_{i\to l}(E) \times Z_{N\to i}(E) \times (\Lambda_N/\lambda_N) \quad \times \Phi_N(E,0)$$

$$\text{Prompt Lepton} \leftarrow \text{Decay} \leftarrow \text{Produce} \leftarrow \text{Attenuate} \leftarrow \text{Primary Flux}$$

Reading from right to left, this expression tells us what we have seen in the previous diagram: the primary flux is attenuated, then produces charm particles which decay into prompt leptons (the decay spectrum-weighted moment Z_{il} is related to the decay spectrum df^l/dE_l).

Does it seems that simple? Well, we must first take a look at the many ingredients used in the calculation, considering that there are many possible phenomenological assumptions to be adopted for each.

3 Phenomenology

A preliminary list of parameters involved in the cascade routines leading to the calculation of the prompt flux comprises:

- Primary Spectrum Amplitude N_o and Slope γ
- Nucleonic Inelastic Cross Section $\sigma_{in}^{N-air}(E)$
- Nucleonic Interaction Length $\lambda_N(E)$
- Nucleonic Spectrum-weighted Moment $Z_{NN}(\gamma, E)$
- Nucleonic Attenuation Length $\Lambda_N(E)$
- Charm Inelastic Cross Section $\sigma_{in}^{i-air}(E)$
- Charm Interaction Length $\lambda_i(E)$
- Charm Production Spectrum-weighted Moment $Z_{Ni}(\gamma, E)$
- Three-body Semileptonic Decay Spectrum $\frac{df^l}{dE_l}$
- Charm Decay Spectrum-weighted Moment $Z_{il}(\gamma)$
- Charm Decay Length d_i

It is up to the user to choose a desired brand for each ingredient. As an example, consider some charm production models found in the literature:

Quark Gluon String Model (QGSM) - A semi-empirical model of charm production based on the non-perturbative QCD calculation by Kaidalov and Piskunova[10], normalized to accelerator data, and applied to the prompt muon calculation by Volkova *et al.*[11].

Recombination Quark Parton Model (RQPM) - A phenomenological non-perturbative approach, taking into account the contribution of the intrinsic charm to the production process, in which a $c\bar{c}$ pair is coupled to more than one constituent of the projectile hadron, as described by Bugaev *et al.*[12].

Perturbative QCD (pQCD) - There are several calculations based on perturbative QCD, for example Thunman *et al.*[13] evaluate explicitly the charm production up to leading order (LO) in the coupling constant, using the Monte Carlo program PYTHIA, and include the next-to-leading order (NLO) distribution effects as an overall factor. More recently Gelmini *et al.*[14] updated the calculation to include the full contribution of NLO predictions to the lepton fluxes. Pasquali *et al.*[15] offer an alternative implementation of the perturbative QCD approach.

Limiting Conditions - E. Zas *et al.*[16] calculate extreme cases of charm production, at both low and high production rate limits. Higher rates are achieved assuming a charm production cross section which is 10% of the total inelastic cross section (called Model-A), extrapolated with a $\log^2(s)$ energy dependence. Lower rates are obtained using pQCD at NLO, with structure functions given by Kwiecinski-Martin-Roberts-Stirling and adopting relatively hard parton distribution functions (called Model-E).

Prompt muon fluxes calculated assuming these charm production models are compared in Figure 2. (The fluxes are multiplied by E^3 in order to flatten the curves.) Two calculations of the conventional atmospheric muon flux are also included, and we note that the cross-over of the conventional and prompt components may occur at any energy between 2×10^3 GeV and 2×10^6 GeV. The prompt flux intensity, itself, spans up to four orders of magnitude! However, we call attention to the fact that the comparison is somewhat unfair, since not only different charm production models are being compared: calculations of different authors involve different assumptions for the other cascading ingredients, so that we are seeing a combination of effects.

Ref.[9] discusses the influence of each separate ingredient upon the final prompt flux, adopting diverse parametrizations available in the literature. For example, the solely effect of the primary cosmic-ray spectrum is displayed in Figure 3. Curves in a) show the spectrum at the top of the atmosphere, according to 5 models. Curves in b) are the corresponding prompt muon-neutrino vertical flux at sea level. Same comparison can be made, fixing all ingredients but the charm production spectrum-weighted moment. The resulting muon-neutrino fluxes for 5 different parametrizations of charm model are shown in Figure 4.

We can think now of mixing different parametrizations of all ingredients listed previously. It is possible to choose extreme combinations, that is to say, those leading to lower and higher prompt lepton fluxes, for a given charm model. This procedure can alter the flux which has been reported in the literature: Figure 5 shows how the calculation of Volkova *et al.* can be shifted down and how the calculation of Thunman *et al.* can be shifted up, by adopting different ingredients, other then the charm model. With the same procedure, Figure 6 shows how the calculation of Bugaev *et al.* wiggles!

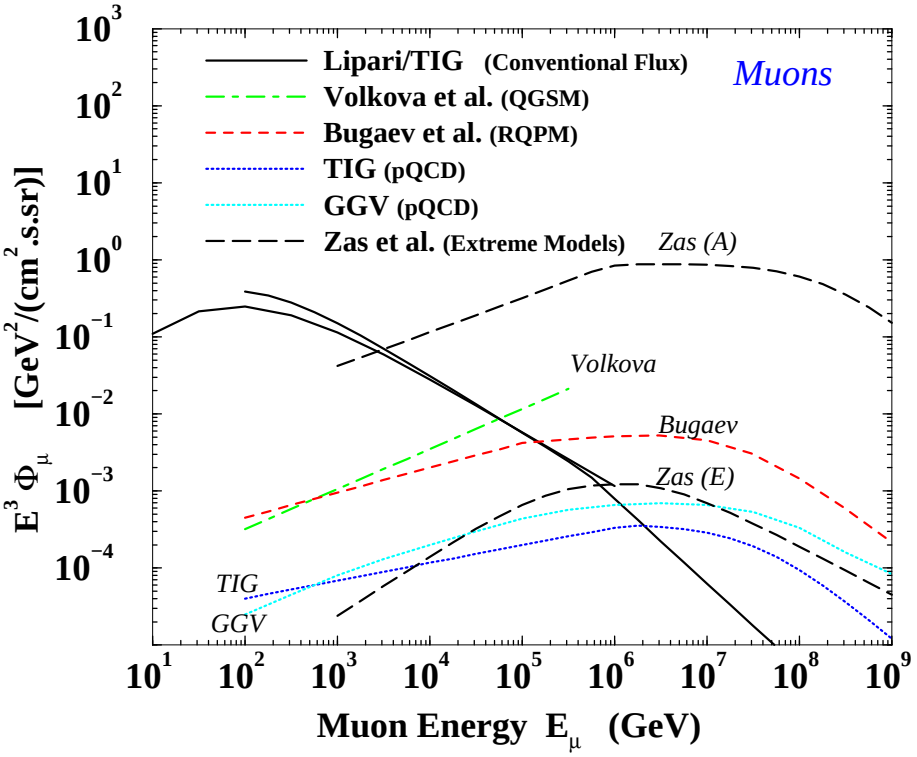

Fig. 2. Comparison of calculated differential vertical atmospheric muon fluxes at sea level, as reported by several authors (see text).

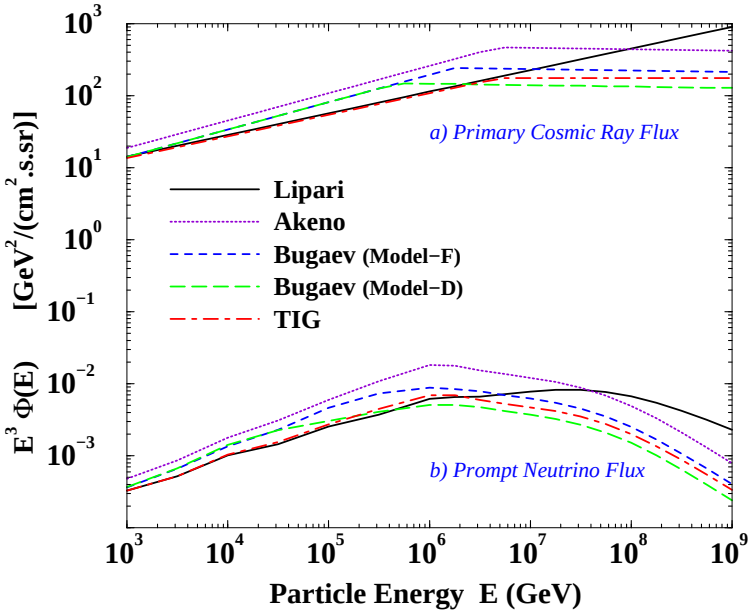

Fig. 3. a) Comparison of primary cosmic-ray energy spectra, as given by different parametrizations ; b)comparison of corresponding prompt neutrino fluxes, assuming all the ingredients fixed but the primary spectrum.

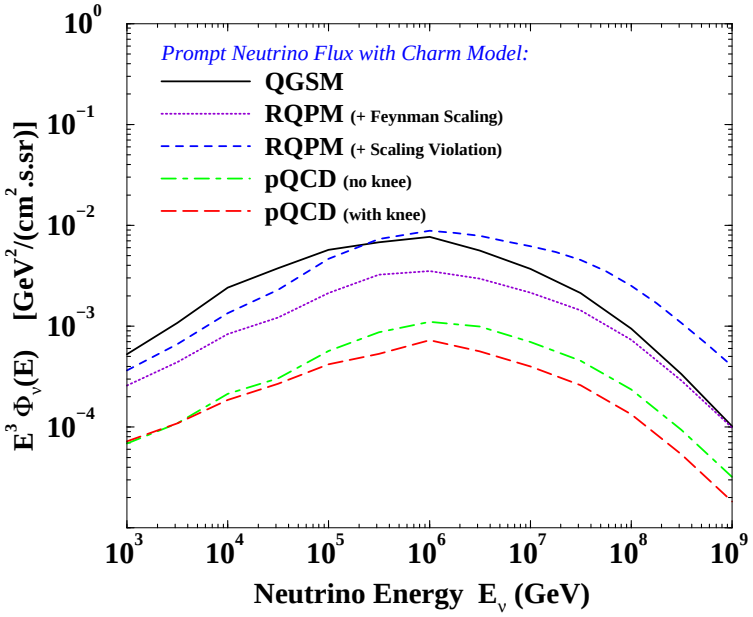

Fig. 4. Comparison of prompt neutrino fluxes for different charm Z-Moment models, assuming all the other ingredients fixed.

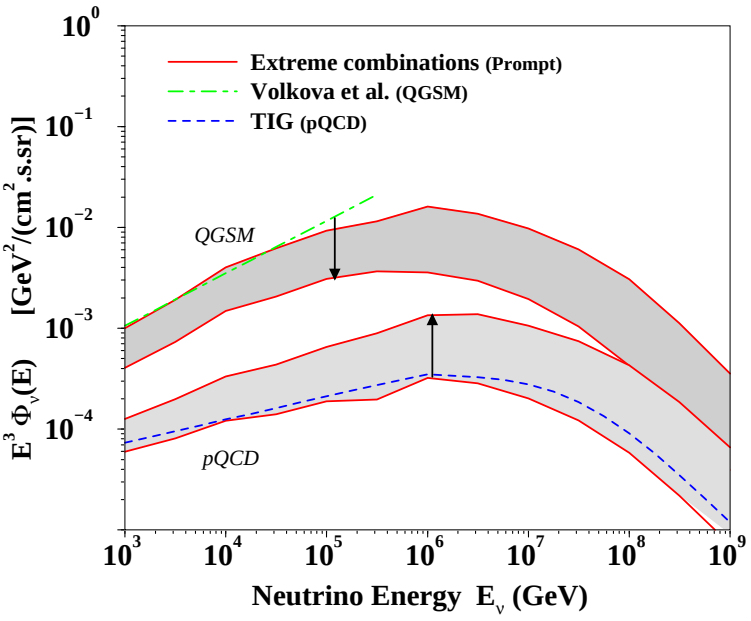

Fig. 5. Prompt neutrino flux calculated with QGSM (upper band) and with pQCD (lower band). The bands represent the range between extreme ingredient combinations, for each charm model. Prompt flux from Volkova *et al.* (dotted line) and from Thunman *et al.* (dot-dashed line) also shown for illustration.

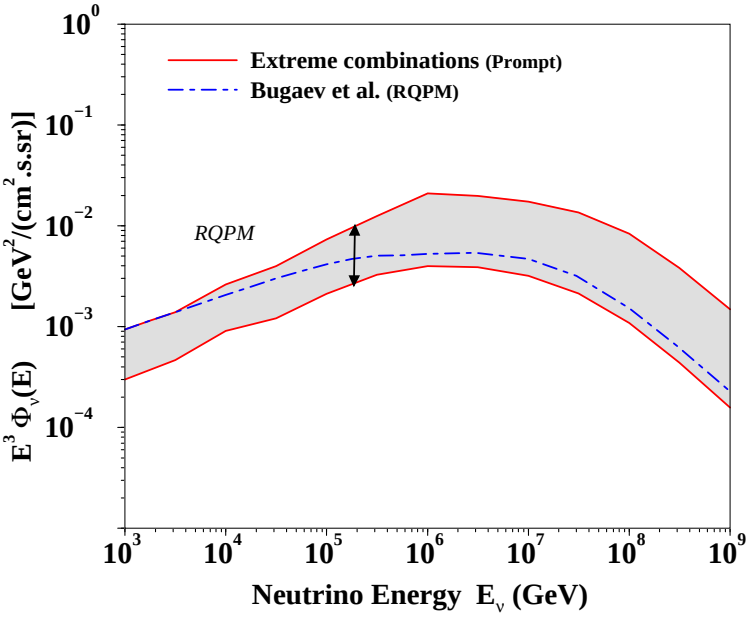

Fig. 6. Prompt neutrino flux calculated with RQPM. The band represents the range between extreme ingredient combinations. Prompt flux from Bugaev *et al.* (dot-dashed line) also shown for illustration.

4 Implications

We have seen how the prompt flux calculation is subjected to large uncertainties, resulting from the imprecise knowledge of both atmospheric particle showering parameters and the modeling of the production of charm. We observe that the calculated neutrino fluxes may be shifted by up to one order of magnitude for a given charm model. When comparison is made among alternative charm production models, the spread reaches two orders of magnitude. We will therefore define an allowed range between the maximum (MAX) and minimum (MIN) prompt neutrino fluxes. The MAX combination of ingredients adopts the QGSM below the knee and the RQPM above, in addition to other extreme parameters. The MIN combination adopts the pQCD charm model, with ingredients that pulls the flux down (complete description of choices is listed in Ref.[9]).

It is not difficult to extend the previous calculation to obtain the flux of prompt tau-neutrinos, the main contribution coming from decay of D_s-mesons into a $\tau\nu$-pair, and subsequent in-chain tau decays producing more neutrinos[18]. The above mentioned conclusions on the uncertainties of the calculation still hold for the tau component.

Applying the prescription of Gandhi *et al.*[17], we can use the calculated fluxes (of prompt ν_μ and ν_τ) to estimate the rates of neutrino-induced muons and taus, per year per effective detection area (in 2π sr), in operating and proposed neutrino telescopes. Table 2 summarizes the event rates for BAIKAL NT-200[3], which have an effective area of 2×10^3 m^2, for AMANDA-II[2], with effective area of 3×10^4 m^2, and for two different thresholds in the proposed km^3 experiment ICECUBE[19]. The estimates for the conventional atmospheric neutrino component (CONV) are shown for comparison. Experimental signatures may come to the rescue on disentangling the two components. For example, the $\approx$ 1,500 prompt ν_μ's above 1 TeV in ICECUBE data may be extracted using their flat zenith angular distribution (while the conventional flux has a strong angular dependence). Prompt ν_τ's would produce characteristic showers in the detector, enabling discrimination of the $\approx$ 200 (20) neutrino induced taus above 1 (10) TeV.

The next question is how the conventional and prompt atmospheric fluxes compare to expected rates of extragalactic neutrinos[5]. Adopting for comparison the upper bound to the diffuse flux of high-energy neutrinos from cosmic accelerators, such as active galactic nuclei and gamma-ray bursts, we summarize the situation for muon-neutrinos in Figure 7. The bands are the allowed region for prompt neutrinos as in Figures 5 and 6. Also shown is the conventional atmospheric flux. Concerning extraterrestrial neutrinos, the two upper curves, labeled MPR (solid and dotted lines), represent the bounds imposed to neutrino fluxes from sources that are optically thick or thin to the emis-

sion of neutrons[20], respectively. The two straight lines labeled WB (dashed and long–dashed), represent bounds on sources which produce the highest energy cosmic rays[21]. The higher flux allows for cosmological evolution of the sources. We observe, from Figure 7, that the prompt neutrino flux exceeds the conventional at some energy above 20 TeV. If the MPR bounds are to hold, the prompt component is merely a background to be discounted. However, according to the WB-scenario, the prompt component may exceed the extragalactic diffuse flux up to 300 TeV, if the sources are to evolve, and up to 2 PeV if not.

Allowing for flavor oscillation of atmospheric and extragalactic muon-neutrinos into tau-neutrinos, Figure 7 can be transformed into Figure 8, remarking that prompt ν_τ's are directly produced from D_s decays and are independent of oscillation mechanisms. Once again we observe the possibility that there is an observational window opened for the prompt component, this time for tau-neutrinos, extending from 2 TeV up to 40 TeV (or up to 500 TeV, depending on the scenario).

Table 2
Upward-going muon and tau event rates per year arising from charged current interactions of atmospheric neutrinos in ice or water, for different neutrino telescope's effective areas and thresholds. Prompt flux calculation based on maximum (MAX) and minimum (MIN) range limits described in the text, compared to conventional atmospheric flux (CONV).

		$\mu^+ + \mu^-$		$\tau^+ + \tau^-$	
Experiment	CONV	Prompt MAX	Prompt MIN	Prompt MAX	Prompt MIN
BAIKAL NT-200	22	3	0	0	0
AMANDA-II	330	44	2	7	0
ICECUBE (> 1 TeV)	11000	1470	53	216	11
ICECUBE (> 10 TeV)	170	157	3	22	1

5 Conclusion

The calculation of the prompt lepton flux in the atmosphere is subjected to large uncertainties. Partially because of our imprecise knowledge of certain atmospheric particle showering parameters. Further uncertainty is associated with the extrapolation to high energy of a variety of models describing the accelerator data on charm production. Care must be taken when comparing results from different calculations, for the combination of ingredients may shift the fluxes up or down.

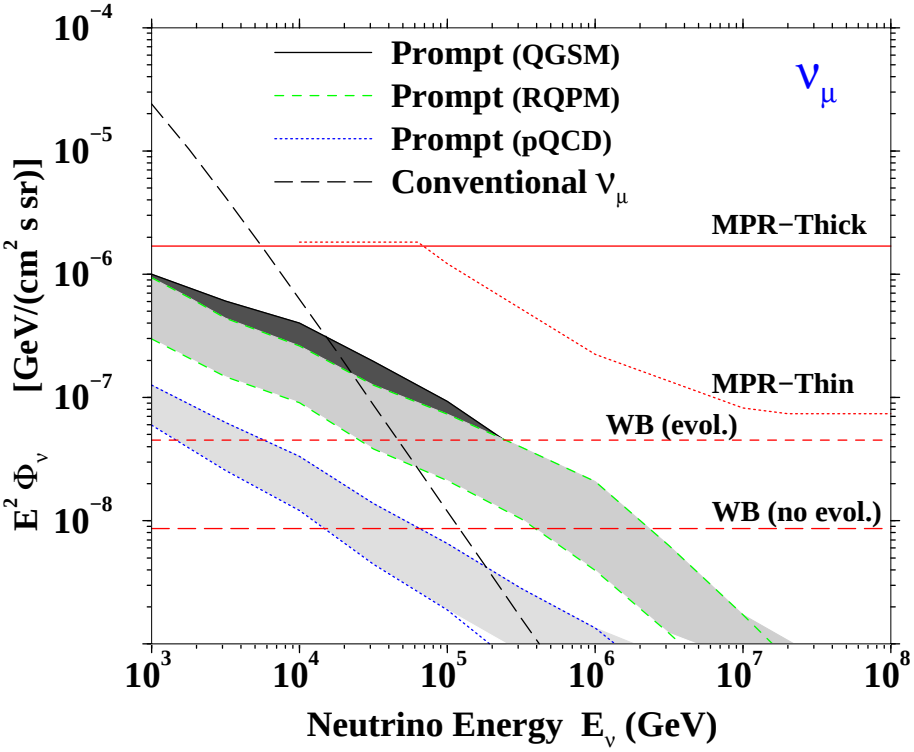

Fig. 7. Comparison of several contributions to the high-energy ν_μ flux. The bands represent the allowed range between maximum and minimum atmospheric prompt neutrino fluxes for different charm production models. Thick dashed line is the conventional atmospheric flux. Solid, dotted, dashed and long-dashed lines correspond to upper bounds imposed to diffuse extragalactic neutrino flux by the observation of high-energy cosmic-ray and gamma-ray spectra, according to different scenarios explained in the text. Fluxes are multiplied by E^2.

Once the uncertainties are quantified, in terms of an allowed band for the prompt atmospheric neutrino flux, we come to the result that prompt neutrinos may be observable in a kilometer-scale neutrino telescope. Actually, it may be possible that a small component of prompt neutrinos are already present in the observed samples of the ongoing experiment AMANDA, given their current limit on the atmospheric neutrino flux[2]. Of course, the existence of a direct observational window for prompt neutrinos depends on the actual bounds to extragalactic neutrino fluxes and, in the case of tau-neutrinos, on the actual values of the flavor oscillation parameters, which are currently subjects of great interest and of intense research.

The actual measurement of prompt neutrinos, and even the failure to do so, will certainly impose constrains to the charm production cross section, at energy domains not yet accessible to particle colliders[6].

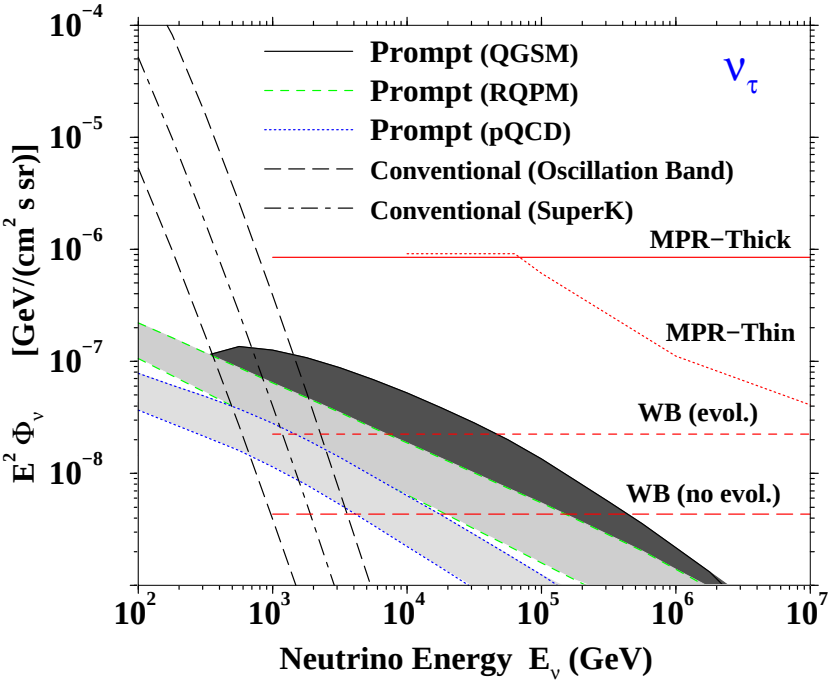

Fig. 8. Comparison of several possible contributions to the high-energy ν_τ flux. Again, the bands represent the allowed range between maximum and minimum atmospheric prompt neutrino fluxes for different charm models. Thick dashed lines are the result of maximum mixing flavor oscillation of the conventional atmospheric ν_μ flux, for Δm^2 around the Super-Kamiokande value 3.2×10^{-3} eV^2(thick dot-dashed line). Solid, dotted, dashed and long-dashed lines correspond to the upper bounds in Figure 7, subjected to vacuum flavor oscillation, averaged in transit to Earth.

Acknowledgements

The authors would like to thank Jean-Marie Frère (ULB) and Daniel Bertrand (IIHE) for support and encouragement. CGSC would like to thank Francis Halzen for the kind hospitality during the "PHENO 2001 Symposium", in Madison, Wisconsin. This work was partially supported by the I.I.S.N. (Belgium) and by The Communauté Française de Belgique - Direction de la Recherche Scientifique, programme ARC.

References

[1] The conventional atmospheric lepton flux has been extensively studied, see for example: E.V. Bugaev and V.A. Naumov, Phys. Lett. B **232,** 391 (1989); P. Lipari, Astropart. Phys.**1,** 195 (1993); M. Honda *et al.*, Phys. Rev. D **53,** 4985 (1995); V. Agrawal *et al.*, Phys. Rev. D **53,** 1314 (1996); G. Battistoni *et al.*, Astropart. Phys.**12,** 315 (2000).

[2] E. Andres *et al.* (The AMANDA Collaboration), Astropart. Phys. **13,** 1 (2000); Nucl. Phys. B (Proc. Suppl.) **91,** 423 (2001); Nature **410,** 441 (March 22, 2001).

[3] V.A. Balkanov *et al.* (The BAIKAL Collaboration), Astropart. Phys. **14,** 61 (2000); Nucl. Phys. B (Proc. Suppl.) **91,** 438 (2001).

[4] See for example Proceedings of TAUP99, Nucl. Phys. B (Proc. Suppl.) **87,** (2000); and of NEUTRINO2000, Nucl. Phys. B (Proc. Suppl.) **91,** (2001).

[5] C.G.S. Costa, F. Halzen and C. Salles, "The prompt TeV-PeV atmospheric neutrino window," preprint ULB-TH/01-08, MADPH/01-1221, hep-ph/0104039.

[6] C.G.S. Costa, F. Halzen, C. Salles and Z. Wlodarczyk, "Is there a large diffractive charm component in high energy particle interaction?" (in preparation).

[7] M.C. Gonzales-Garcia, F. Halzen, R.A. Vázquez and E. Zas, Phys. Rev. D **49,** 2310 (1994).

[8] G. Gelmini, P. Gondolo and G. Varieschi, Phys. Rev. D **61,** 056011 (2000). Phys. Rev. D **63,** 036006 (2001).

[9] C.G.S. Costa, Astropart. Phys. (to be published, 2001), hep-ph/0010306.

[10] A.B. Kaidalov and O.I. Piskunova, Z. Phys. C **30,** 145 (1986).

[11] L.V. Volkova *et al.*, Nuovo Cimento C **10,** 465 (1987). For a recent discussion see T.S. Sinegovskaya and S.I. Sinegovsky, Phys. Rev. D **63,** 096004 (2001).

[12] E.V. Bugaev *et al.*, Nuovo Cimento C **12,** 41 (1989); Phys. Rev. D **58,** 054001 (1998).

[13] M. Thunman, G. Ingelman and P. Gondolo, Astropart. Phys. **5**, 309 (1996).

[14] G. Gelmini, P. Gondolo and G. Varieschi, Phys. Rev. D **61**, 036005 (2000).

[15] L. Pasquali, M.H. Reno and I. Sarcevic, Phys. Rev. D **59**, 034020 (1999).

[16] E. Zas, F. Halzen and R.A. Vázquez, Astropart. Phys. **1,** 297 (1993).

[17] R. Gandhi, C. Quigg, M.H. Reno and I. Sarcevic, Phys. Rev. D **58**, 093009 (1998).

[18] L. Pasquali and M.H. Reno, Phys. Rev. D **59,** 093003 (1999).

[19] F. Halzen *et al.*, in *Proceedings of the 26th International Cosmic Ray Conference,* South Lake City (USA), edited by D. Kieda, M. Salamon and B. Dingus, Vol. 2, 428-431 (1999); C. Spiering, Nucl. Phys. (Proc. Suppl.) **91,** 445 (2001).

[20] K. Mannheim, R.J. Protheroe and J.P. Rachen, astro-ph/9908031 (1999); Phys. Rev. D **63**, 023003 (2000).

[21] E. Waxman and J. Bahcall, Phys. Rev. D **59**, 023002 (1999); hep-ph/9902383 (2000).